Nonlinear System Identification of a Riveted Beam using a Hilbert Transform Based Approach

Suzanna Gilbert
Graduate Research Assistant; Brigham Young University – Mechanical Engineering Department
gsuzi26@student.byu.edu

Matthew S. Allen
Professor; Brigham Young University – Mechanical Engineering Department
matt.allen@byu.edu

Brandon Rapp
Senior Principal Structures Engineer; Pratt & Whitney
brandon.rapp@prattwhitney.com

Abstract

Structures with mechanical joints display complicated, hysteretic behavior that can be difficult to characterize using existing nonlinear system identification techniques. However, methods based on the Hilbert Transform have been successful in several previous works. In this work, a Hilbert Transform-based approach is used with impact measurements to determine the amplitude-dependent modal parameters of a slender riveted beam which has similar features to a component on an aircraft engine. An impact at almost any point on the beam excites several modes, most of which exhibit varying levels of nonlinearity and decay at varying rates. Additionally, because the structure is light, one cannot apply a large number of accelerometers and use a modal filter because this would add significant cable damping to the structure. This paper presents the results of system identification on this structure, in the presence of these features that push the limits of the Hilbert Transform method.

Keywords: contact nonlinearity, system identification, rivets

1. Introduction

Mechanical joints are of great interest in dynamics research because they are widely used and are usually the main source of damping and nonlinearity in built-up structures. This nonlinearity is a result of slip within the joint interface, which changes the stiffness of the joint and adds damping from friction. The amount of slip depends on the deflection shape of the modes and their amplitudes of vibration. Thus, jointed structures exhibit a type of nonlinearity where the modal frequencies and damping ratios shift as a function of vibration amplitude. It is useful to quantify this behavior to better understand the dynamics of the system and to enable more accurate prediction of the stresses experienced by the system, thereby allowing one to develop more efficient designs. For example, one could take advantage of the added damping from joint friction instead of assuming linearity and over-building the structure to provide sufficient strength.

Many nonlinear system identification methods have been proposed and are often validated on simple benchmark structures or models. However, most system identification techniques have

weaknesses that make them difficult to use or unreliable when applied to structures with joints. Thus, the selection of a proper method for a given system is a challenge in and of itself. One method that has been particularly useful is Feldman's "Freevib" method [1], which uses the Hilbert transform of the transient ringdown of a system to extract the amplitude-dependent frequency and damping of each mode. This method has proven effective in several studies [2]. It does not require extensive measurements; the instantaneous modal parameters can be extracted from a single ring-down. No previous knowledge of the system is required, and it can be applied to a wide variety of linear and nonlinear systems. However, a major drawback of the Hilbert transform approach is that it is only valid for mono-component signals. Thus, the individual modes must first be isolated. This becomes difficult in highly nonlinear systems where there are significant interactions between modes and other features such as nonlinear harmonics. Popular techniques for separating out modes for Hilbert processing are bandpass filtering, modal filtering [3] and empirical modal decomposition [4]. The latter is combined with the Hilbert transform in the Hilbert-Huang transform.

However, this class of techniques does have limitations. Jin et. al. found evidence that the Hilbert transform method performs more poorly for systems with greater nonlinearity; in a numerical study with a duffing oscillator, the Hilbert transform showed greater error in identifying the stiffness and damping as the amplitude of the nonlinear stiffness term increased relative to the linear stiffness [5]. Prior studies that used it successfully [3] treated systems with damping nonlinearities rather than the stiffness nonlinearity studied by Jin et al. The Hilbert transform is known to be sensitive to noise because it involves taking derivatives of the amplitude and phase; thus, smoothing or curve-fitting are usually applied to the signal and the way that this is done certainly affects the results. The algorithm also introduces end effects into the signal, often requiring truncation of the beginning and end of the signal. Other similar methods are the zero-crossing method [6] and the peak finding and fitting algorithm [7], both of which estimate the instantaneous frequency and damping of a single mode from a ring-down measurement, and thus share the requirement to isolate an individual mode.

In this work, a system identification approach based on the "Freevib" method is used to identify the amplitude-dependent frequency and damping of a riveted beam. The results are used in a companion paper [8] to update and validate a finite element model of the structure.

The riveted beam is comprised of two long, thin steel beams connected along their length by 24 rivets in two offset rows, such that the contact area extends along the entire length of the structure. The beam offers a unique challenge for system identification; the contact area plays a larger role in the beam dynamics than many benchmark structures or industrial equipment, and its thin, lightweight frame requires a measurement setup that does not add significant mass or damping to the structure.

This research constitutes a first attempt to understand the behavior of this structure. It also provides another experimental example of applying the Hilbert transform to assess the nonlinear behavior of a jointed structure, supplementing the lessons learned in prior studies [3], [9], [10]. However, the riveted beam exhibits stronger nonlinearity than most, if not all, of the systems studied in previous works of this type. The results of this experiment reveal interesting dynamic

behavior of the riveted beam, as well as limitations in the Hilbert transform's ability to characterize a system with significant contact nonlinearity.

2. Method

The riveted beam is pictured in Figure 1 (a). The specimen was hung from bungees placed approximately at the nodes of the first mode of the beam to simulate free-free boundary conditions. Two uniaxial accelerometers were placed in the corners at one end of the beam as shown in Figure 1 (b). No accelerometers were attached to the top edge of the beam, because each half of the beam is too narrow to individually support an accelerometer without it touching the other half (see Figure 1 (c)). Although a triaxial accelerometer could have measured the vibration in the y-direction, the triaxial accelerometer available was significantly more massive and has a stiffer, more massive cable, both of which would potentially shift the modal properties of the beam. Thus, the stiff-direction (y-direction) bending modes were not captured in these measurements. Further, adding several more accelerometers to the beam to enable modal filtering, as has been done in similar works [3], [11], [12] would add significant cable damping to this lightweight structure; thus modal filtering is not employed in this work.

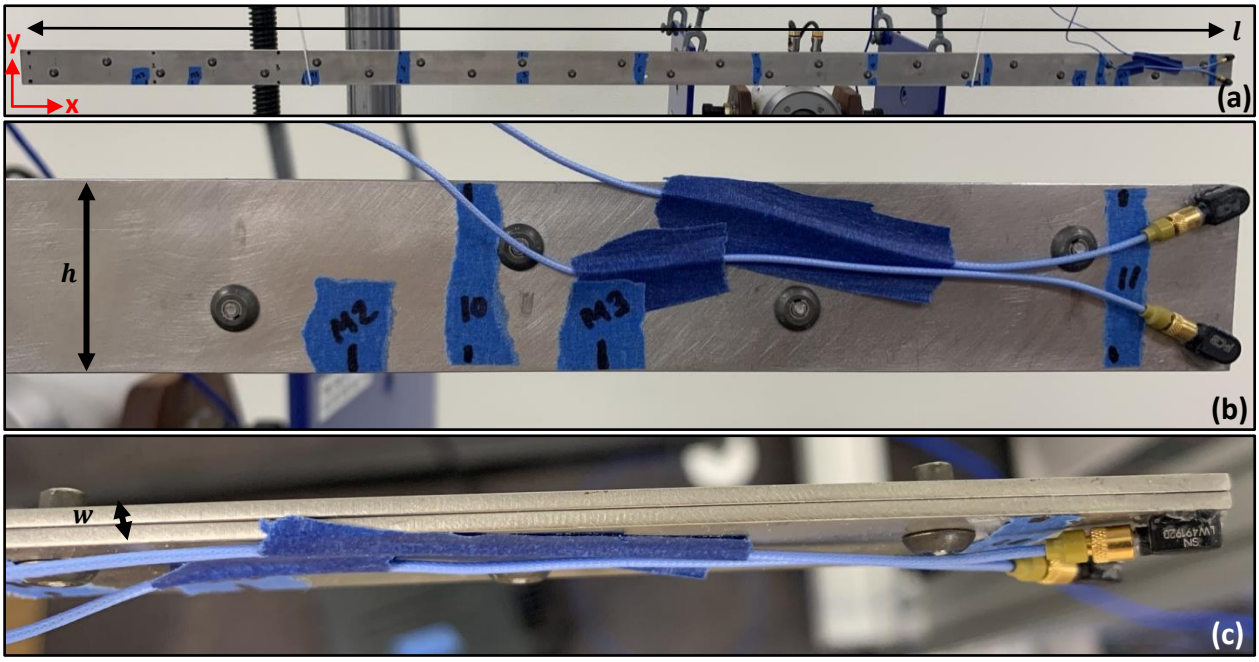

Figure 1. (a) Riveted beam hung from bungees, (b) accelerometer setup at right end of beam, and (c) top view of beam showing both halves riveted together.

First, the linear natural frequencies and mode shapes were obtained from a roving hammer test at very light impact levels, to identify modes of interest for nonlinear testing and select appropriate drive points to excite the desired modes. The rigid body modes of the beam-bungee setup were also measured to confirm that they do not interfere with the flexural modes; the highest rigid body mode was at 23% of the first bending mode frequency, low enough to easily separate with a bandpass filter but not quite low enough to meet Carne's 10x separation rule [13] which ensures that it does not affect the accuracy with which one can measure the bending mode. Hence, the

bungees were placed at the nodes of the first bending mode in an attempt to further decouple it from the rigid body motions.

Following the linear test, nonlinear impact testing was performed at higher excitation forces to record the nonlinear transient decay. The drive points shown in Figure 2 were chosen to excite the first 6 modes of the beam, all of which were found to exhibit significant nonlinearity. Table 1 summarizes the drive points used for each mode. A wide range of impact force levels was used, from about 1 N to 300 N. This is because the nonlinearity of each mode is excited at very different amplitudes. As will be shown later, an impact force that causes significant shifts in damping and frequency for the sixth mode will barely affect the first and second modes.

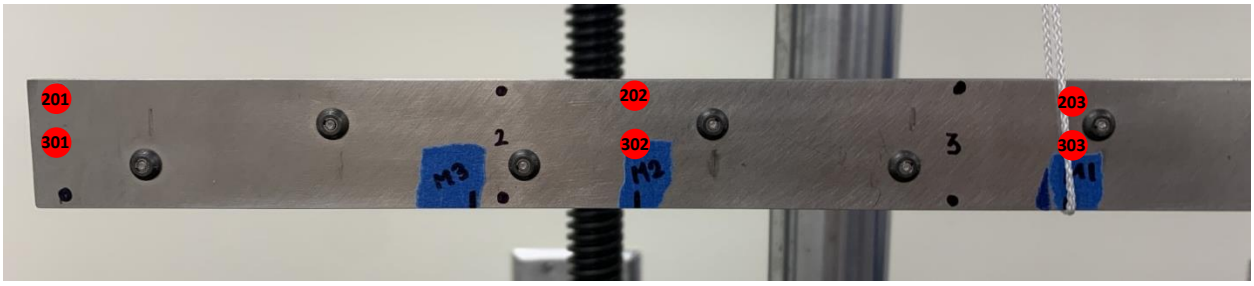

Figure 2. Drive point locations for nonlinear impact tests are indicated by the red dots.

Table 1. Drive points used for each mode

Mode	Drive Points Used
1	201, 301, 302
2	201, 301, 303
3	201, 301, 302, 303
4	201, 202, 302, 303
5	201, 202, 302, 303
6	201, 203

The amplitude-dependent frequency and damping for each mode was obtained using a Hilbert transform algorithm as set forth in detail in [10], [14] and summarized here. One exception is that modal filtering is not employed, as mentioned previously, because only two accelerometers are used. Instead, the torsion modes are separated from the bending modes by combining the accelerometer signals appropriately. If a_1 and a_2 are the top and bottom accelerometers respectively, then the torsion modes are suppressed by averaging the two signals as in Equation 1 and are accentuated by taking the difference of the two signals as in Equation 2.

$$y_b = \frac{a_1 * a_2}{2} \quad (1)$$

$$y_t = \frac{a_1 - a_2}{2} \quad (2)$$

This is especially helpful when the torsion modes are close in frequency to the bending modes. Once the bending and torsion modes are separated, the modes are well-spaced enough to isolate by applying a third or fourth-order bandpass filter to the signals. For example, Figure 3 shows

the FFT of the response after a filter was applied to Mode 2, with the blue showing the measured, average accelerometer response (Eqn. 1) and the red showing the same after applying the filter.

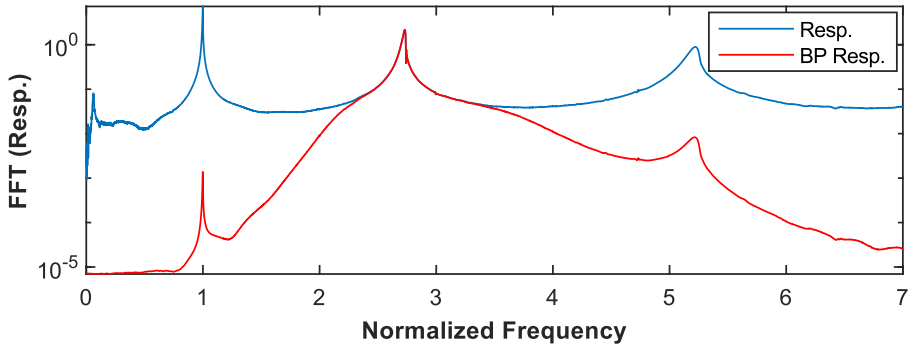

Figure 3. Bandpass filter (red) applied to the FFT (blue) to isolate bending Mode 2.

The Hilbert transform was then applied to the filtered signal to obtain the time-varying amplitude and phase during ringdown. The phase and amplitude envelope were then manually curve-fit by choosing time values along the envelope (shown by the "endpoints" in Figure 4) and applying a piecewise linear fit (green lines in Figure 4) where each linear line segments falls between a pair of "endpoints". The piecewise linear functions can be differentiated to obtain the frequency and damping versus time (as elaborated in [15]). These can then be used to obtain the frequency and damping ratio as a function of vibration amplitude for this mode (blue curves in Fig. 4).

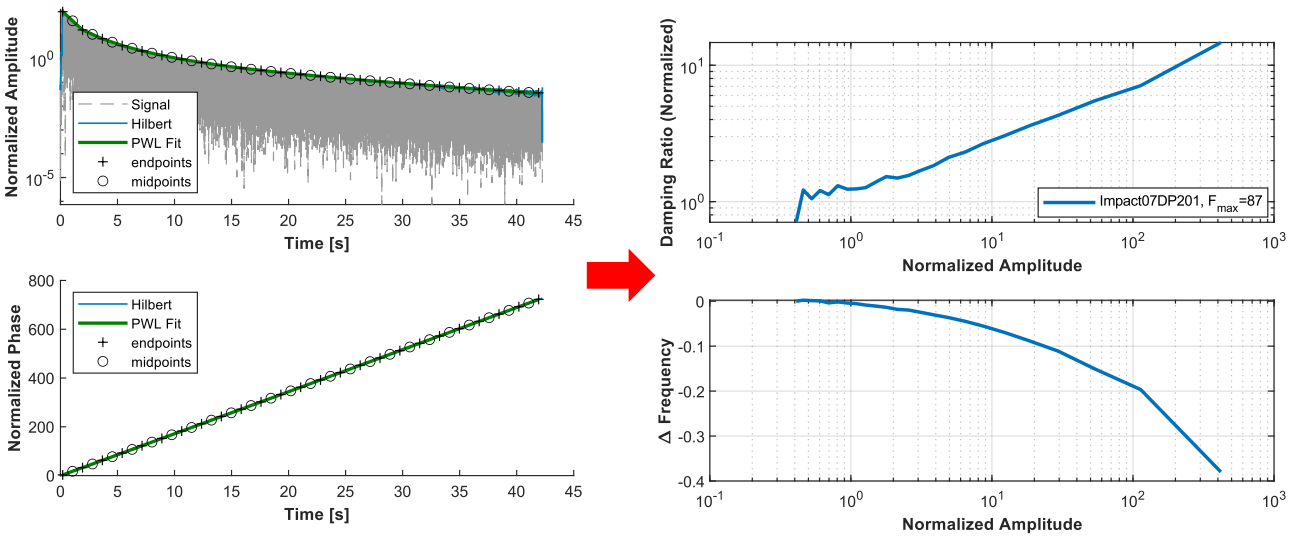

Figure 4. Piecewise linear fit (PWL) applied to the amplitude envelope and phase of the signal (left), and the resulting frequency shift and normalized damping ratio vs normalized amplitude (right).

3. Results & Discussion

The acceleration response from a single impact reveals several modes, most of which are well-spaced. The first seven are shown in the frequency response function (FRF) in Figure 5 and listed in Table 2. This work focuses on only the first 6 modes. One can see that as mode order increases, the amount of nonlinearity and damping increases as well. Therefore, higher impact forces are needed to investigate the nonlinear range of the first couple modes, and lower force levels are needed for the fourth through sixth modes. The FRF shown here was obtained from an impact force of 23 N, which excites minimal nonlinearity in the first three modes and significantly affects everything above Mode 4. The curve shown comes from only the bottom accelerometer (a_2) where both bending and torsion are visible. The first five modes captured are out-of-plane bending modes. This excludes the first stiff-direction (or in-plane) bending mode, which was not measured, but falls between the third and fourth out-of-plane bending modes. The sixth mode is the first torsion mode; however, this mode swaps order with the fifth bending mode at forcing levels of greater than about 10 N, due to a strong stiffness nonlinearity that causes a large frequency shift. Thus, in Figure 5 the sixth mode shows up as the fifth peak.

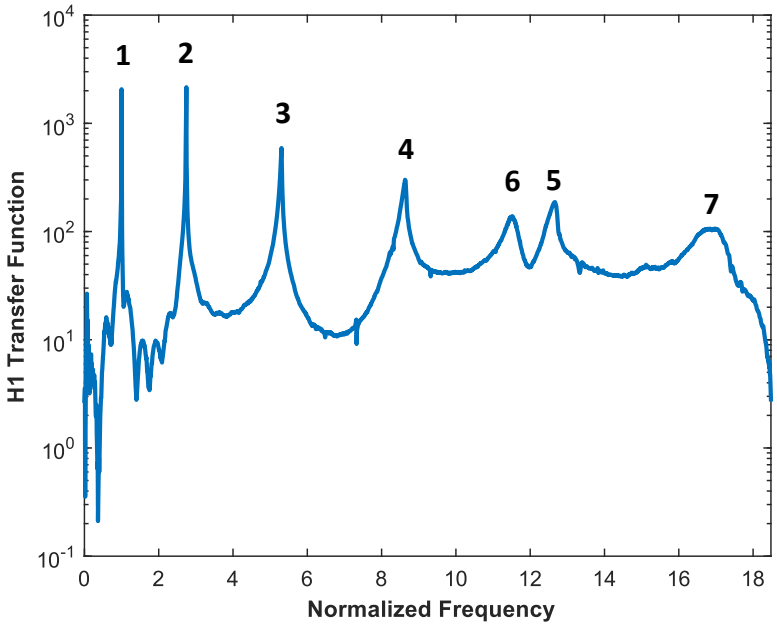

Figure 5. FRF (H1 estimate) calculated from the response of the bottom accelerometer (a_2) and the impact force from a 23 N impact, showing the first seven modes of the beam. The frequency is normalized by the first mode frequency.

Table 2. First seven modes of riveted beam with their deflection type and normalized linear frequency.

Mode #	Normalized Linear Frequency	Mode Type
1	1.00	Bending
2	2.75	Bending
3	5.32	Bending
---	~8.46	Stiff Bending

4	8.69	Bending
5	12.80	Bending
6	13.41	Torsion
7	17.46	Bending

Figure 6 shows the relative position of the fifth bending and first torsion modes for three impact force levels: 7 N, 16 N, and 198 N. The dramatic frequency shift of the first torsion mode means that at some amplitudes, Modes and 5 and 6 are very close or exactly on top of each other, making them impossible to separate with a bandpass filter. Although these modes can be separated by either averaging or differencing the accelerometer signals, the torsion signal still contains a small response at the frequencies of the bending modes. The frequency range of the bandpass filter must also be monitored and adjusted to account for the large frequency shifts in these modes. This makes the process less automated and more time-consuming.

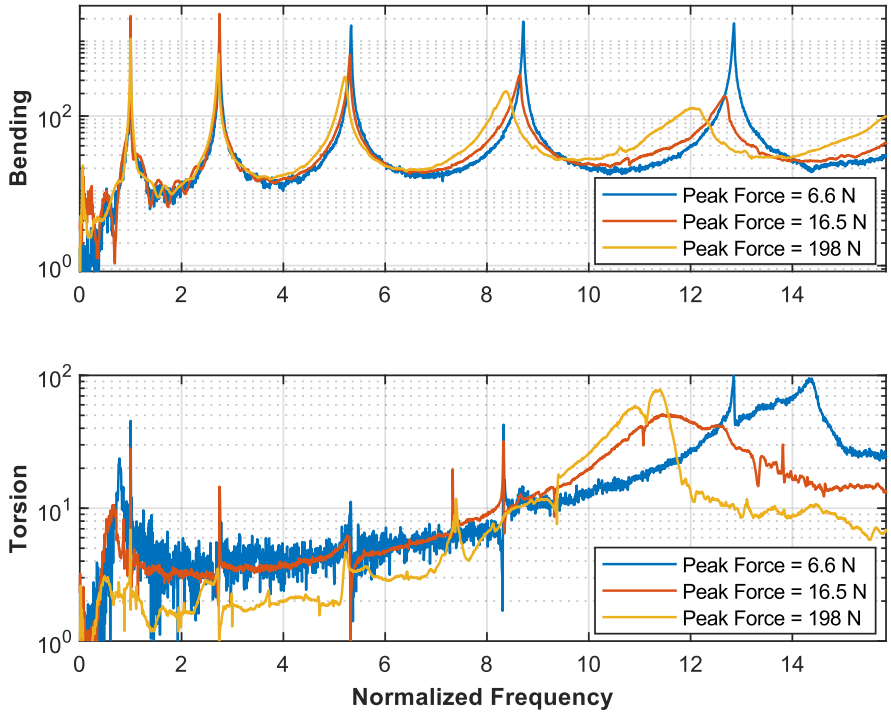

Figure 6. FFTs showing the first 5 modes visible in the bending mode signal y_b in Eqn. (1) and first torsion mode from the torsion signal y_t in Eqn. (2) for three different excitation levels.

As mentioned, after isolating the torsion mode per Eqn. (2), there is still some energy from the bending modes left in the signal, showing up as small peaks at the frequencies of the bending modes (see Figure 6). Although small, these small peaks can have a significant effect on the Hilbert transform analysis of the sixth mode if they are not eliminated by the bandpass filter. The bending modes are not as heavily damped as the torsion mode and have longer decay times. Thus, even though they show up at relatively small amplitudes, at some point in the transient ringdown they will dominate the decay envelope after the torsion mode has decayed to a low enough amplitude. This becomes an issue when Modes 5 and 6 are close enough that they cannot

be separated with a bandpass filter. Figure 7 shows what the decay envelope looks like in this case and the resulting frequency and damping curves. The decay rate of the envelope changes abruptly when the fifth bending mode (denoted by the green arrow) becomes dominant, and the resulting damping and frequency see a corresponding jump. The frequency jumps from the value of the fifth bending mode at low amplitudes (shown in green), to the value for the first torsion mode at high amplitudes (yellow). When this occurs, the jump in the frequency and damping is avoided by only curve-fitting the higher-amplitude end of the envelope (the yellow section) where the mode of interest is dominant. This limits the low end of the amplitude range for which the frequency and damping of this mode can be extracted.

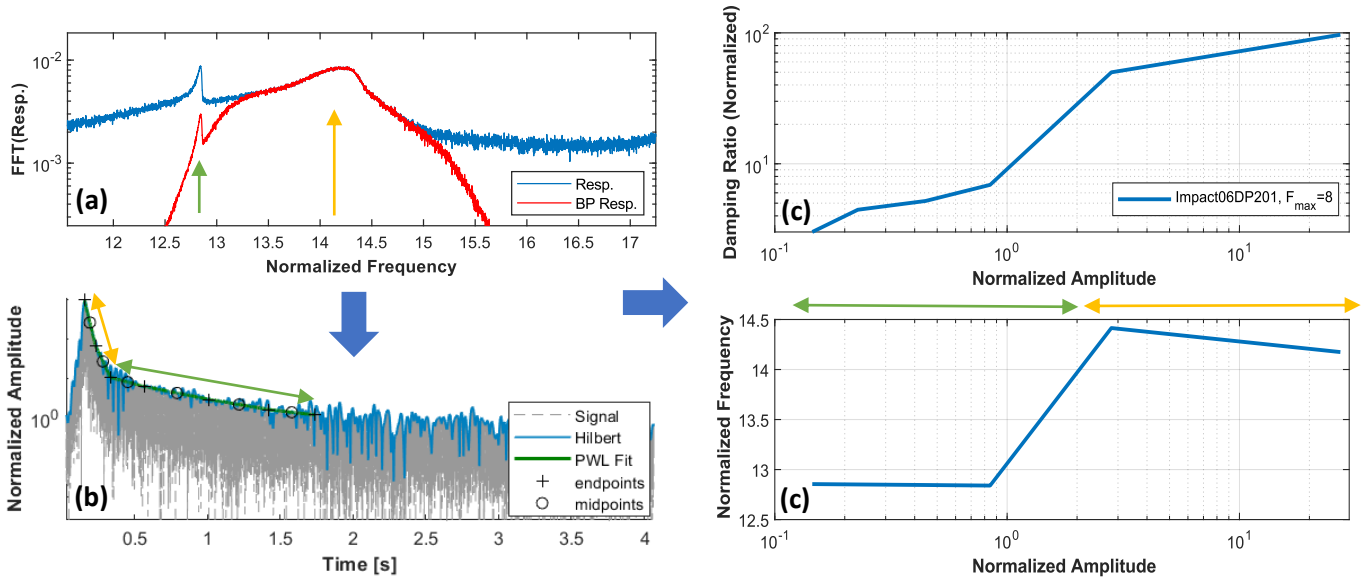

Figure 7. (a) Bandpass filter picking up more than one mode, (b) the amplitude envelope of the filtered signal, and (c) the corresponding damping and frequency extracted from the amplitude and phase. The first torsion mode is pointed out by the yellow arrows, and the fifth bending mode by the green arrows.

The amplitude range that can be obtained is also limited on the high end. At high vibration amplitudes, many of the peaks become heavily damped, as depicted in Figure 8(a). These highly damped peaks are not large compared to nearby modes and other noisy artifacts in the signal. The high damping also results in very quick decay times, insomuch that the startup transient introduced by the filter is present for the majority of the decay, adding error to the estimated damping. The filter effect shows up as small ripples at the beginning of the amplitude envelope (before 29s) in Figure 8(b). Both the filter effects and other sources of noise make this mode difficult or impossible to curve-fit without capturing too much of the noise, which greatly impacts the estimated damping.

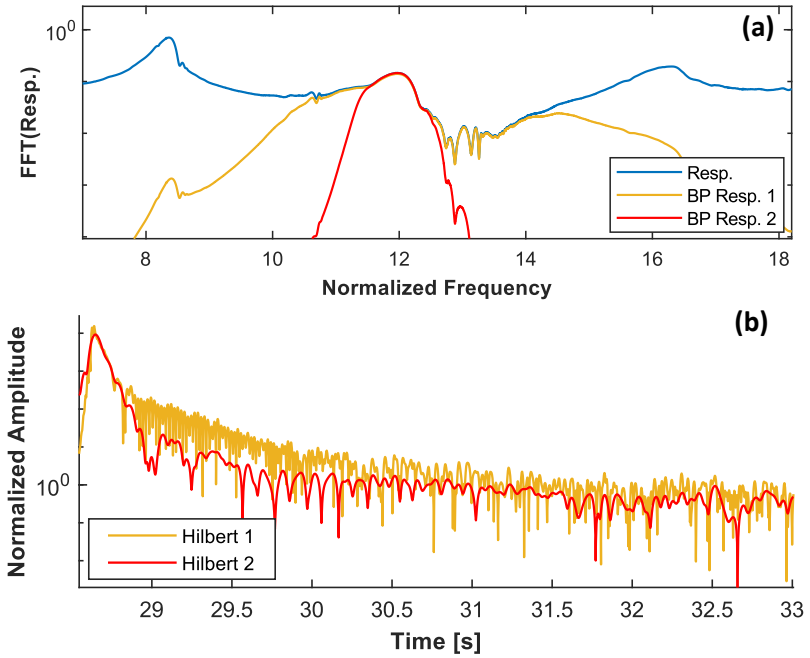

Figure 8. (a) Bandpass filters of two different widths applied to a highly damped Mode 5, and (b) the resulting amplitude envelopes.

Despite the above-mentioned limitations, the Hilbert Transform method was able to produce the frequency and damping versus amplitude for each of the first 6 modes, which are shown in Figure 9. Each curve in Fig. 9 comes from a different impact, with the color denoting the drive point used. Each mode shows a softening linearity with a downward frequency shift that increases with mode order. For example, for an impact force of 198 N, the frequency shift increases from less than 1 Hz for Mode 1, to 14 Hz for Mode 5. Mode 6 has a much more dramatic frequency shift, which is greater than 50 Hz for the same impact force level. Frequency shifts this large do not show up in Fig. 9(l) because no impacts of this force level were able to be processed successfully using the Hilbert transform, due to the limitations discussed earlier in this section. However, larger frequency shifts show up in the FFT (see Fig. 6). The damping ratio increases with amplitude, with a uniform shift of about one order of magnitude across the first 6 modes. However, the baseline, or linear, damping increases about an order of magnitude between Modes 1 and 6 as well.

The results for Mode 1 are quite good (see Fig. 9(a-b)), showing consistency over a wide range of impact force levels (from 20 to 167 N). The curves start to spread apart at their high-amplitude end however. Mode 2 exhibits significantly more spread, where the frequency and damping of the individual curves converge to different values, and Modes 3 through 6 continue to show a large spread as well as a considerable amount of noise.

The noise is a direct result of trying to extract damping and frequency from a noisy phase and amplitude envelope, such as that shown in Figure 8(b). Compare Mode 3 with Mode 2 in Figure 9, where Mode 3 is much noisier than Mode 2. Also notice that the noisier curves tend to come from higher amplitude impacts, when the modes become heavily damped and decay quickly, as

discussed earlier. For example, in Fig. 9(g), the curves coming from impact forces of less than 11 N appear cleaner (less jagged) than those from the higher impact levels.

Even more noticeable is the spread in the frequency and damping, where each curve decays to a different value, giving the curves the appearance of being stacked on top of one another. The variation in damping levels between the curves can be up to half the damping shift seen in an individual curve. A similar comparison exists for the frequency curves. One potential cause for this spread is modal coupling, a nonlinear phenomenon where the modes influence each other. Because the force in the joints depends on the deflection shapes of all the modes, each mode's effective frequency and damping can change due to the other modes. This is evidenced by the fact that Mode 1 shows very little coupling, except at the ends. Mode 1 takes much longer to decay than the higher modes, as shown in Figure 10. In fact, each consecutive mode decays more quickly than the previous mode. Because Mode 1 has a much longer decay time, at some point all of the modes except for Mode 1 will have decayed to a low enough amplitude and not contribute any more to the frequency and damping of Mode 1 (for example, after 7s in Fig. 10). At this point, the spread in Mode 1 disappears. Mode 2 shows significantly more coupling (Fig. 9 (c-d)), as Mode 1 is active during the entire decay period of Mode 2. However, when the drive point is chosen to be on the nodal line of Mode 1, suppressing Mode 1, the spread in Mode 2 almost entirely disappears. The blue curves in Figure 9 correspond to this drive point. For Modes 3 and above, no drive point was able to suppress Modes 1-2 when testing Mode 3, nor Modes 1-3 when testing Mode 4, and so on. If one were to plot the modes of a free-free beam, which this structure approximates, one could show that there is no single point that suppresses both Modes 1 and 2, or any combination of the first 3 modes. However, some drive points are still able to reduce the coupling more than others, i.e. the blue curves in the Mode 3 plots and the pink curves in the Mode 4 and 5 plots.

Another clue pointing to modal coupling is that the height of each curve appears to depend on impact force level. The harder impacts tend to produce the curves with higher levels of damping and greater downward frequency shifts; thus the individual curves become sorted in order of impact force level, even though the impacts were delivered in no particular order with respect to force level. Higher impact forces not only put more energy into the mode of interest, but into the other modes as well, which collectively increase the force in the joint and consequently, increase the damping and frequency shift observed in the mode of interest.

It is also known that jointed structures can exhibit variability when the joint slips and then sticks again in slightly different positions from test to test so that the contact stresses change between tests. This is referred to as residual tractions [16], [17], and is a potential contributor to the variability seen in the results here.

The purpose of these measurements is to provide accurate experimental data to update and validate a finite element model of the riveted beam [8]. It is far easier to simulate an uncoupled response, for example by using QSMA [11] which solves for each mode individually. Thus, it is desirable to provide experimental data with minimal modal coupling. Looking again at Figure 9, the curves with the lowest damping or highest frequency presumably are the least affected by mode coupling. Unfortunately, these curves usually come from the lightest impacts, and thus are limited to lower amplitudes where less nonlinearity is present.

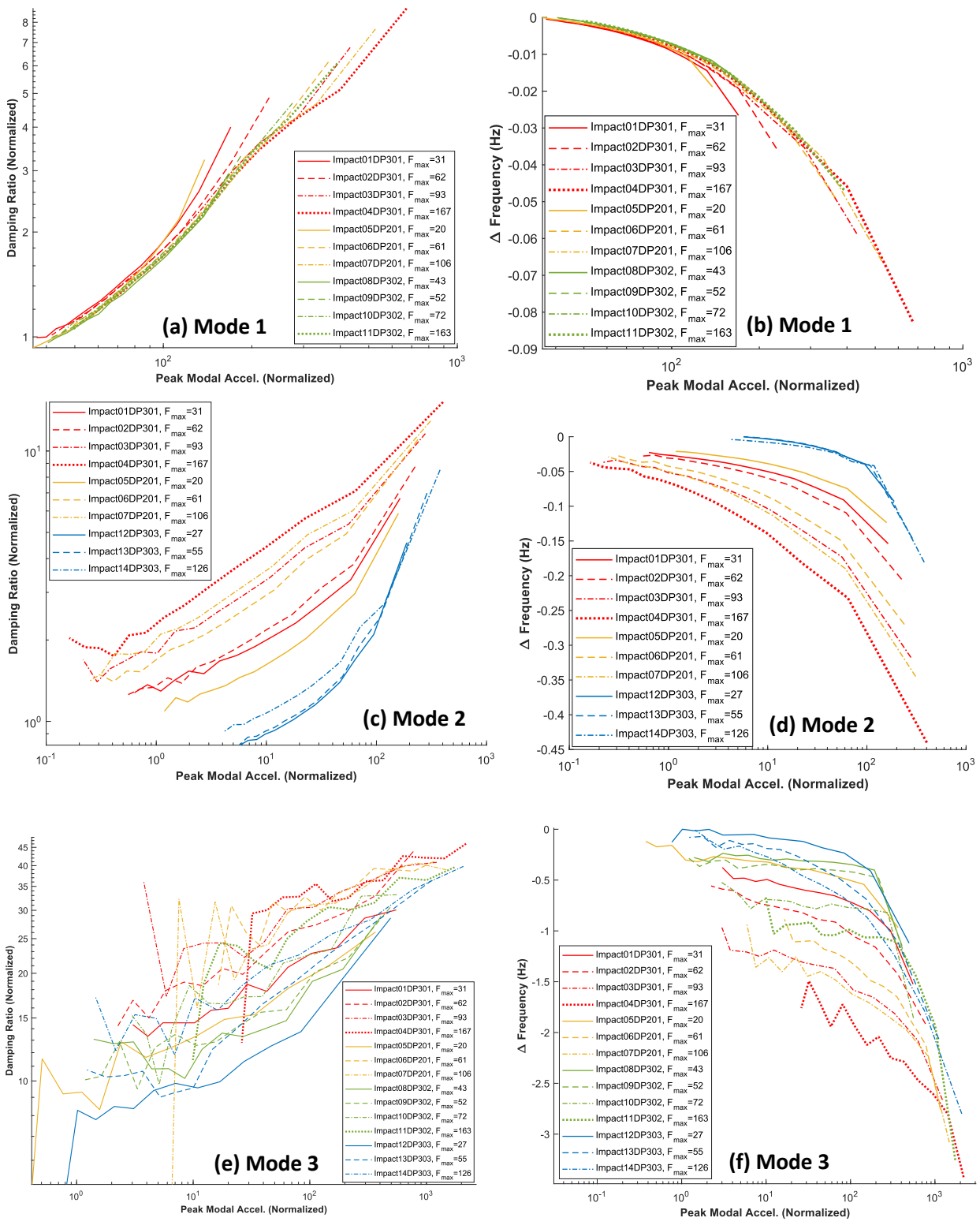

Figure 9 Part I. Normalized damping ratio and frequency shift (in Hz) vs normalized amplitude for the first 3 bending modes.

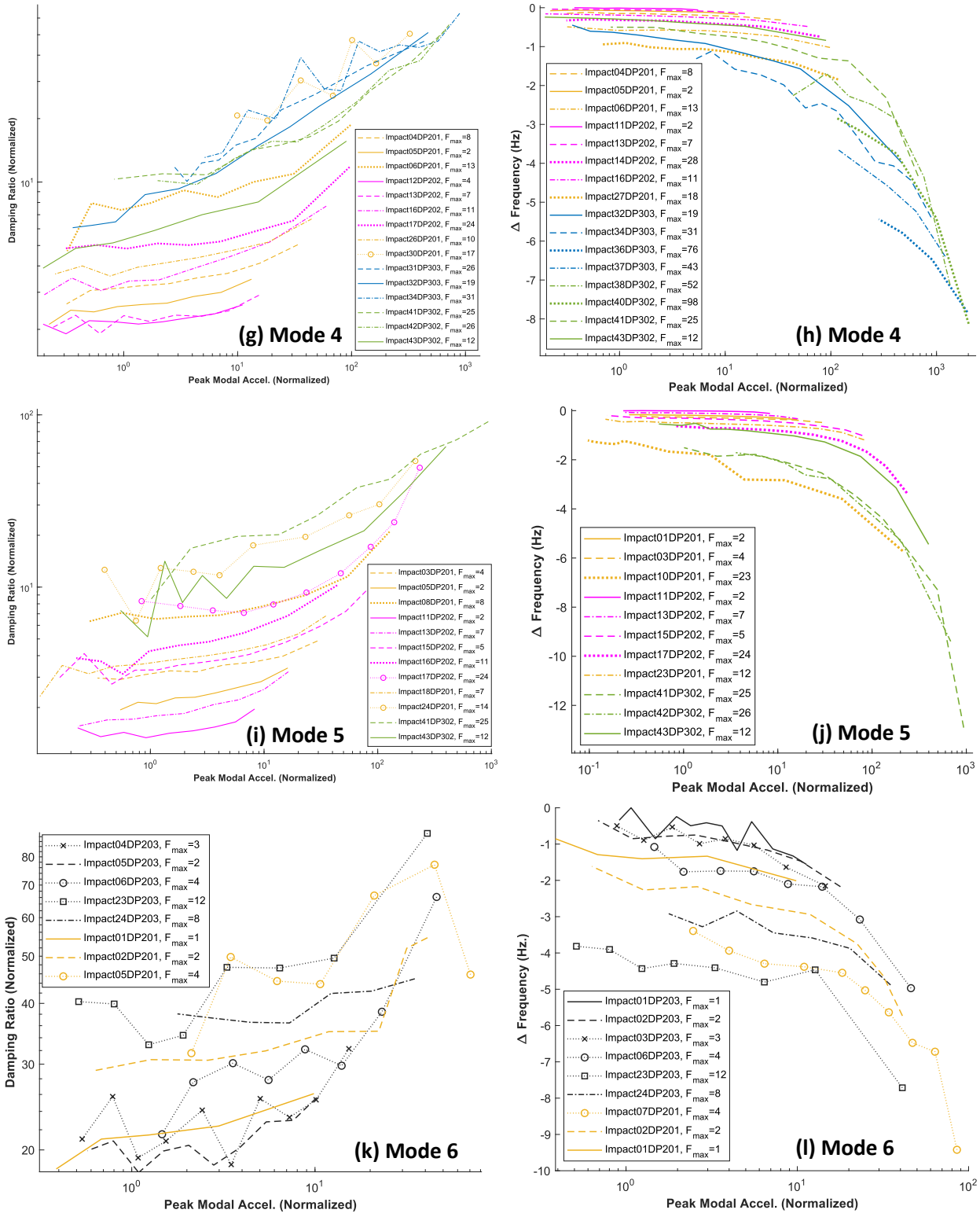

Figure 9 Part II. Normalized damping ratio and frequency shift (in Hz) vs normalized amplitude for Modes 4-6.

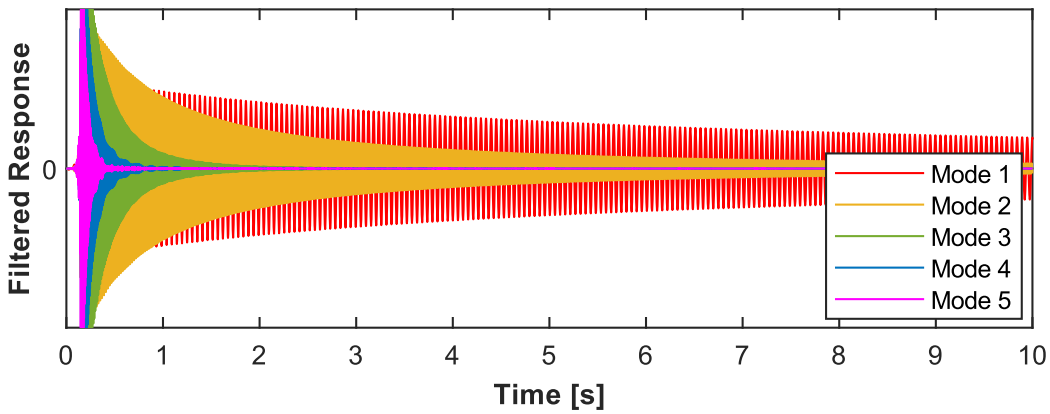

Figure 10. Filtered time response of the first five modes in a single impact.

4. Conclusion

This study used a Hilbert-transform based system identification method to calculate the amplitude-dependent frequency and damping of six modes on a riveted beam. The beam response was found to contain several modes with greatly varying levels of nonlinearity, as well as frequency shifts large enough for modes to swap order. Large variation was observed in the damping and frequency of almost all the modes, likely due to modal coupling. System identification on this beam highlights some of the challenges associated with applying the Hilbert transform method to a system exhibiting highly nonlinear modes, modal interactions, and closely-spaced modes. Despite these challenges, the amplitude-dependent frequency and damping were calculated for all six modes. However, as mode order increases, the amplitude range that can be analyzed becomes increasingly limited. At high excitation levels, many of the modes become so highly damped that they are difficult to distinguish from noise and are dominated by filter effects; higher excitation levels also cause more modal interactions, which is not ideal for model updating. For some modes, the lower amplitude end of the ring-down becomes dwarfed by more dominant modes nearby. This is a limitation introduced by using a bandpass filter to separate modes.

Future work includes trying new measurement techniques and postprocessing strategies. Measurement methods based on shaker excitation can target a single mode and may be able to reduce modal interactions significantly. A more rigorous filtering process, such as that proposed in [7] may help to reduce the influence of the filter, allowing data with very sharp decay rates to be extracted more accurately. A system identification method that can fit multiple modes at once, such as simultaneous time-fitting [18] may be more successful at dealing with the closely-spaced modes observed in this work.

References

[1] M. Feldman, “Non-linear system vibration analysis using Hilbert transform--I. Free vibration analysis method ‘Freevib,’” *Mech. Syst. Signal Process.*, vol. 8, no. 2, pp. 119–127, Mar. 1994, doi: 10.1006/mssp.1994.1011.

[2] G. Kerschen, K. Worden, A. F. Vakakis, and J.-C. Golinval, “Past, present and future of nonlinear system identification in structural dynamics,” *Mech. Syst. Signal Process.*, vol. 20, no. 3, pp. 505–592, Apr. 2006, doi: 10.1016/j.ymssp.2005.04.008.
[3] A. Singh *et al.*, “Experimental Characterization of a New Benchmark Structure for Prediction of Damping Nonlinearity,” in *Nonlinear Dynamics, Volume 1*, G. Kerschen, Ed., Cham: Springer International Publishing, 2019, pp. 57–78. doi: 10.1007/978-3-319-74280-9_6.
[4] N. E. Huang *et al.*, “The empirical mode decomposition and the Hilbert spectrum for nonlinear and non-stationary time series analysis,” *Proc. R. Soc. Lond. Ser. Math. Phys. Eng. Sci.*, vol. 454, no. 1971, pp. 903–995, Mar. 1998, doi: 10.1098/rspa.1998.0193.
[5] M. Jin, M. R. W. Brake, and H. Song, “Comparison of nonlinear system identification methods for free decay measurements with application to jointed structures,” *J. Sound Vib.*, vol. 453, pp. 268–293, 2019, doi: https://doi.org/10.1016/j.jsv.2019.04.021.
[6] J. M. Londoño, S. A. Neild, and J. E. Cooper, “Identification of backbone curves of nonlinear systems from resonance decay responses,” *J. Sound Vib.*, vol. 348, pp. 224–238, 2015, doi: https://doi.org/10.1016/j.jsv.2015.03.015.
[7] M. Jin, W. Chen, M. R. W. Brake, and H. Song, “Identification of Instantaneous Frequency and Damping From Transient Decay Data,” *J. Vib. Acoust.*, vol. 142, no. 051111, Jun. 2020, doi: 10.1115/1.4047416.
[8] Josh Blackham, Cameron Stoker, Matthew S. Allen, and Brandon Rapp, “Nonlinear Model Updating for Riveted Joints,” in *Proceedings of IMAC XLIII*, Orlando, Florida, Feb. 2025.
[9] M. R. W. Brake, C. W. Schwingshackl, and P. Reuß, “Observations of variability and repeatability in jointed structures,” *Mech. Syst. Signal Process.*, vol. 129, pp. 282–307, Aug. 2019, doi: 10.1016/j.ymssp.2019.04.020.
[10] D. R. Roettgen and M. S. Allen, “Nonlinear characterization of a bolted, industrial structure using a modal framework,” *Mech. Syst. Signal Process.*, vol. 84, pp. 152–170, Feb. 2017, doi: 10.1016/j.ymssp.2015.11.010.
[11] R. M. Lacayo and M. S. Allen, “Updating structural models containing nonlinear Iwan joints using quasi-static modal analysis,” *Mech. Syst. Signal Process.*, vol. 118, pp. 133–157, Mar. 2019, doi: 10.1016/j.ymssp.2018.08.034.
[12] M. Wall, M. S. Allen, and R. J. Kuether, “Observations of modal coupling due to bolted joints in an experimental benchmark structure,” *Mech. Syst. Signal Process.*, vol. 162, p. 107968, Jan. 2022, doi: 10.1016/j.ymssp.2021.107968.
[13] T. G. Carne, D. Todd Griffith, and M. E. Casias, “Support conditions for experimental modal analysis,” *Sound Vib.*, vol. 41, no. 6, Art. no. 6, 2007.
[14] M. W. Sracic, M. S. Allen, and H. Sumali, “Identifying the modal properties of nonlinear structures using measured free response time histories from a scanning laser Doppler vibrometer,” presented at the 30th International Modal Analysis Conference, Jan. 2012.
[15] B. J. Deaner, M. S. Allen, M. J. Starr, and D. J. Segalman, “APPLICATION OF VISCOUS AND IWAN MODAL DAMPING MODELS TO EXPERIMENTAL MEASUREMENTS FROM BOLTED STRUCTURES,” 2013.
[16] E. Ferhatoglu, J. Groß, and M. Krack, “Frequency response variability in friction-damped structures due to non-unique residual tractions: Obtaining conservative bounds using a nonlinear-mode-based approach,” *Mech. Syst. Signal Process.*, vol. 201, p. 110651, Oct. 2023, doi: 10.1016/j.ymssp.2023.110651.

[17] A. Klarbring, “Examples of non-uniqueness and non-existence of solutions to quasistatic contact problems with friction,” *Arch. Appl. Mech.*, vol. 60, pp. 529–541, Jan. 1990, doi: 10.1007/BF00541909.
[18] A. Singh, “Simultaneous Direct Time Fitting of a Multi-Mode Response to Determine the Instantaneous Frequency and Damping,” in *International Modal Analysis Conference XLI - Austin, Texas, United States of America - February - 2023*, US DOE, Feb. 2023. doi: 10.2172/2431989.